# Dilepton production at CMS LHC: inverse gluon and photon emission vs the Drell–Yan process and photon fusion

V. A. Zykunov (JINR, GSU)

Quarks–2026, XXIII International Seminar on High-Energy Physics

Petrozavodsk, Russia,
18 – 23 May, 2026

# Introduction

Despite the fact that the Standard Model (SM) keeps the status of consistent and experimentally confirmed theory, the search of New Physics

- **the supersymmetry**,
- **M-theory**,
- **DM-particles**,
- **axions**,
- **feebly interacting particles**,
- **extra** spatial dimensions,
- **extra** neutral gauge bosons, etc.

is continued.

One of powerful tool in the modern experiments at LHC is the investigation of **dilepton production**

$$pp \to \ell^+ \ell^- X, \quad \ell = \mu, e \tag{1}$$

at **large invariant mass** of lepton pair: $M \geq 1$ TeV.

# Current experimental situation at CMS LHC

The measured observable quantities:

- differential cross section $\frac{d\sigma}{dM}$,
- double-differential cross section $\frac{d^2\sigma}{dMdy}$,
- forward-backward asymmetry $A_{FB}$

are consistent with the SM predictions at

- $\sqrt{S} = 7$–$8$ TeV, 19.7 fb$^{-1}$
- $\sqrt{S} = 13$ TeV, 85 fb$^{-1}$
- $\sqrt{S} = 13.6$ TeV, 285.4 fb$^{-1}$ ($\sim$ 10% of Run3)

where $\sqrt{S}$ – total energy in c. m. s. of hadrons, $M$ – dilepton $\ell^+\ell^-$ invariant mass, $y$ – dilepton rapidity.

- NNLO QCD and NLO EW RCs are taken into account by **FEWZ**.

# Four mechanisms of dilepton production

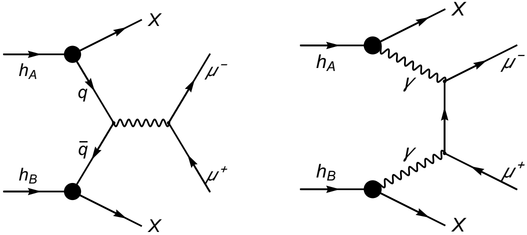


Figure 1: The *Drell–Yan process*, and the *photon-photon* fusion.

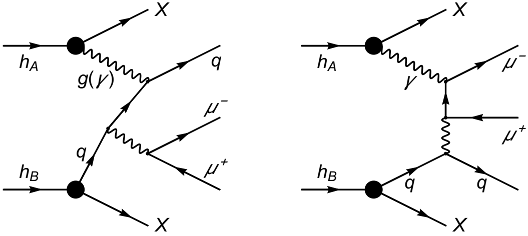


Figure 2: Inverse gluon or $\gamma$ emission with *quark*, and with *muon*.

# Notations: invariants, coupling constants

The standard set of **Mandelstam invariants** for the partonic elastic scattering (with $p_1 + p_2 = p_3 + p_4$):

$$s = (p_1 + p_2)^2, \quad t = (p_1 - p_3)^2, \quad u = (p_2 - p_3)^2. \tag{2}$$

The propagator for $j$-boson depends on its mass $m_j$ and width $\Gamma_j$:

$$D_j(q) = \frac{1}{q^2 - m_j^2 + i m_j \Gamma_j}, \quad j = \gamma, Z. \tag{3}$$

Suitable combinations of coupling constants are:

$$\lambda_{f\,+}^{\,i,j} = v_f^i v_f^j + a_f^i a_f^j, \quad \lambda_{f\,-}^{\,i,j} = v_f^i a_f^j + a_f^i v_f^j, \tag{4}$$

$$v_f^\gamma = -Q_f, \quad a_f^\gamma = 0, \quad v_f^Z = \frac{I_f^3 - 2 s_W^2 Q_f}{2 s_W c_W}, \quad a_f^Z = \frac{I_f^3}{2 s_W c_W}.$$

# $q\bar{q}$-annihilation Born: diagrams and cross sections

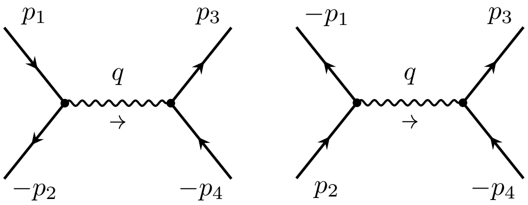


Figure 3: Feynman diagrams of $q\bar{q}(\bar{q}q) \rightarrow \ell^-\ell^+$ process at Born level.

**Partonic level**:

$$d\sigma^0_{q\bar{q}} = \frac{2\pi\alpha^2}{s^2} \sum_{i,j=\gamma,Z} D_i {D_j}^* \sum_{\chi=+,-} {\lambda_q}^{i,j}_{\chi} {\lambda_\ell}^{i,j}_{\chi} (t^2 + \chi u^2) dt. \tag{5}$$

# $\gamma\gamma$-fusion Born: diagrams and cross sections

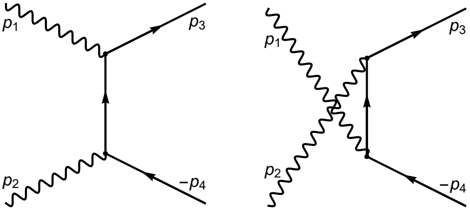


Figure 4: Feynman diagrams of $\gamma\gamma \to \ell^-\ell^+$ process at Born level.

**Partonic level**:

$$d\sigma^0_{\gamma\gamma} = \frac{2\pi\alpha^2}{s^2}\frac{t^2+u^2}{tu}dt. \tag{6}$$

**Hadronic level** ($\mathcal{C} = \cos\theta$):

$$\frac{d^3\sigma^0_h}{dMdyd\mathcal{C}} = 8\pi\alpha^2 f^A_\gamma(x_1) f^B_\gamma(x_2)\frac{t^2+u^2}{SM^5(1-\mathcal{C}^2)}\Theta. \tag{7}$$

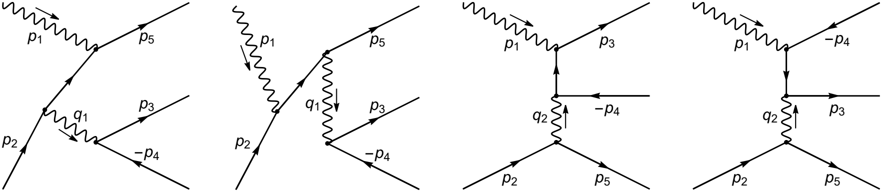


Figure 5: Feynman diagrams of $\gamma q(gq) \to \ell^- \ell^+ q$ process.

**Partonic level**:

$$d\sigma_{\gamma q} = \frac{1}{2^6 \pi^5 s} \sum_{a,b} \overline{\sum_{\text{pol}}} \mathcal{M}^a_{\gamma q} (\mathcal{M}^b_{\gamma q})^+ d\Phi_3. \quad (8)$$

**Hadronic level**:

$$d\sigma^{\text{ex}}_{\gamma q} = \sum_q f^A_\gamma(x_1, Q^2) dx_1 \, f^B_q(x_2, Q^2) dx_2 \, d\sigma_{\gamma q}. \quad (9)$$

# Some details for hadronic cross section

After using quark-parton model rules and some algebra, $j = (q, \ell, q\ell, \ell q)$:

$$d\sigma_j^{\mathrm{ex}} = \frac{\alpha^3 J_x}{\pi^2 s} \sum_q f_\gamma^A(x_1) f_q^B(x_2) \left[ V_j \, S_j^V + A_j \, S_j^A \right] d\Phi_3' \, dMdy, \tag{10}$$

where vector and axial combinations are factorized as following:

$$\begin{aligned} V_q &= Q_q^2 \sum_{a,b=\gamma,Z} \lambda_{qV}^{ab} \lambda_{\ell V}^{ab} D_a(q_1) D_b^*(q_1), \\ V_\ell &= Q_\ell^2 \sum_{a,b=\gamma,Z} \lambda_{qV}^{ab} \lambda_{\ell V}^{ab} D_a(q_2) D_b^*(q_2), \ldots \end{aligned} \tag{11}$$

For Jacobian of transition to experimental variables we have:

$$dx_1 dx_2 = |J_x| dMdy, \quad J_x = \frac{2M\left(E_5 + \sqrt{E_5^2 + M^2}\right)}{S\sqrt{E_5^2 + M^2}}. \tag{12}$$

# Phase space

$$d\Phi_3 = \delta(\ldots)\frac{d^3\mathbf{p_3}}{2E_3}\frac{d^3\mathbf{p_4}}{2E_4}\frac{d^3\mathbf{p_5}}{2E_5} \to \frac{\pi|\mathbf{p_3}||\mathbf{p_5}|}{4E_4\mathcal{F}}d(\cos\theta_3)dE_5 d(\cos\theta_5)d\varphi_5.$$

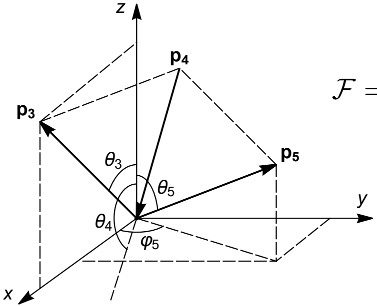


Figure 6: Configuration of final 3-vectors

$$\mathcal{F} = 1 + E_3\left(1 + \mathcal{B}/|\mathbf{p_3}|\right)\left(\mathcal{A} + E_3^2 + 2\mathcal{B}|\mathbf{p_3}|\right)^{-\frac{1}{2}},$$

where coefficients look like

$$\mathcal{A} = m_4^2 - m_3^2 + |\mathbf{p_5}|^2,$$
$$\mathcal{B} = |\mathbf{p_5}|\cos\theta_{35},$$
$$\mathcal{C} = E_1 + E_2 - E_5,$$

$$\cos\theta_{35} = \cos\theta_3\cos\theta_5 + \sin\theta_3\sin\theta_5\cos\varphi_5.$$

$$E_3 = \frac{1}{2(\mathcal{B}^2 - \mathcal{C}^2)}\left(\mathcal{C}(\mathcal{A} - \mathcal{C}^2) + \mathcal{B}\sqrt{(\mathcal{A} - \mathcal{C}^2)^2 + 4m_3^2(\mathcal{B}^2 - \mathcal{C}^2)}\right),$$

# Leading Logarithms (LL) approximation

Photon-quark interaction:

$$p_5 = (1-\eta)p_1, \;\; \eta p_1 + p_2 = p_3 + p_4,$$

$$L_q = \log \frac{4E_5^2}{m_q^2} = \log \frac{M^2(1-\eta)^2}{m_q^2\eta},$$

$$P_{\gamma q} = (1-\eta)^2 + \eta^2,$$

Photon-lepton interaction:

$$p_5 = (1-\eta)p_2, \;\; p_1 + \eta p_2 = p_3 + p_4,$$

$$L_\ell = \log \frac{4E_2^2E_5^2}{m_q^2(E_2-E_5)^2} = \log \frac{M^2(1-\eta)^2}{m_q^2\eta^3},$$

$$P_{\gamma\ell} = [1+(1-\eta)^2]/\eta,$$

where Splitting functions $P_{\gamma j}$ as by **Altarelli & Parisi (1977)**.

LL cross sections:

$$d\sigma_q^{\mathrm{LL}} = \frac{\alpha}{2\pi}\sum_q Q_q^2 \int_0^1 d\eta\, f_\gamma^A(x_1) f_q^B(x_2)\, dx_1 dx_2 L_q P_{\gamma q} J_\eta d\sigma^0_{\bar{q}q}(\eta),$$

$$d\sigma_\ell^{\mathrm{LL}} = \frac{\alpha}{2\pi}\sum_q Q_q^2 \int_0^1 d\eta\, f_\gamma^A(x_1) f_q^B(x_2)\, dx_1 dx_2 L_\ell P_{\gamma\ell} J'_\eta d\sigma^0_{\gamma\gamma}(\eta).$$

# Quark mass Singularity

To solve the problem of quark mass dependance (i. e. quark singularuty, QS) we apply the $\overline{MS}$-subtraction technics – the subtraction from exact cross section (10) the so-called QS-term

$$d\sigma_j^{\mathrm{IE}} = d\sigma_j^{\mathrm{ex}} - d\sigma_j^{\mathrm{QS}},$$

which looks as LL-terms with prescripted substitutions: for quark case

$$d\sigma_q^{\mathrm{QS}} = \frac{\alpha}{2\pi} \sum_q Q_q^2 \log \frac{M^2}{m_q^2} \int_0^1 d\eta \, P_{\gamma q} \, J_\eta \, d\sigma_{\bar{q}q}^0(\eta) f_\gamma^A(x_1) f_q^B(x_2) \, J_x \, dMdy,$$

and for lepton case

$$d\sigma_\ell^{\mathrm{QS}} = \frac{\alpha}{2\pi} \sum_q Q_q^2 \int_0^1 d\eta \, P_{\gamma\ell} \Big( \log \frac{M^2}{m_q^2 \eta^2} - 1 \Big) J'_\eta d\sigma_{\gamma\gamma}^0(\eta) f_\gamma^A(x_1) f_q^B(x_2) \, J_x \, dMdy.$$

# Numbers

It is time to show some numbers. Firstly, main features of EWK and QCD NLO RCs calculation are following:

- The notations, the Feynman rules are inspired by review of **M. Böhm, H. Spiesberger, and W. Hollik, 1986**,
- **the t'Hooft–Feynman gauge**,
- **on-mass renormalization scheme** $(\alpha, \alpha_s, m_W, m_Z, m_H$ and the fermion masses as independent parameters),
- QCD result is obtained from QED one by substitution:

$$Q_q^2 \alpha \to \sum_{a=1}^{N^2-1} t^a t^a \alpha_s = \frac{N^2-1}{2N} I \alpha_s \to \frac{4}{3} \alpha_s, \qquad (13)$$

  here $2t^a$ – Gell-Mann matrices, and $N = 3$,
- **ultrarelativistic approximation** where it is possible.

# Some modern codes for NLO and NNLO RCs for hadronic colliders (in the ABC order)

- DYNNLO (S. Catani, L. Cieri, G. Ferrera et al.)
- FEWZ (R. Gavin, Y. Li, F. Petriello, S. Quackenbush)
- HORACE (C.Carloni Calame, G.Montagna, et al.)
- MCSANC (Dubna: A. Andonov, A. Arbuzov, D. Bardin et al.) (pioneer work on the topic: **A. B. Arbuzov and R. R. Sadykov, JETP 106, 488 (2008)** )
- MC@NLO (S. Frixione, F. Stoeckli, P. Torrielli et al.)
- PHOTOS (N. Davidson, T. Przedzinski, Z. Was et al.)
- POWHEG (L. Barze, G. Montagna, P. Nason et al.)
- RADY (S. Dittmaier, A. Huss, C. Schwinn et al.)
- READY (V. Zykunov, RDMS CMS)
- WINHAC (W. Placzek, S. Jadach, M. W. Krasny et al.)
- ZGRAD (U. Baur, W. Hollik, D. Wackeroth et al.)

# Code READY and a set of prescriptions

In the following the scale of radiative effects to dilepton production will be discussed using FORTRAN program **READY**: (**R**adiative corr**E**ctions to l**A**rge invariant mass **D**rell–**Y**an process).

We used the following set of prescriptions:

- standard PDG set of SM input electroweak parameters,
- "effective" quark masses ($\Delta\alpha^{(5)}_{had}(m_Z^2) = 0.0276$),
- 5 active flavors of quarks in proton,
- CTEQ, MRST'04, CT10, MHHT14 and NNPDF'24 sets of PDFs,
- choice for PDFs: $Q = M_{sc} = M$.

# CMS detector setup

We impose the experimental restriction conditions

- on the detected lepton angle $-\zeta^* \leq \cos\theta \leq \zeta^*$ (or on the rapidity $|y(l)| \leq y(l)^*$); for CMS detector the cut values of $\zeta^*$ (or $y(l)^*$) are determined as

$$\zeta^* \approx 0.986614 \quad (\text{or} \quad y(l)^* = 2.5),$$

- the second standard CMS restriction $p_T(l) \geq 20$ GeV,
- the "bare" setup for muon identification requirements (no smearing, no recombination of muon and photon/gluon).

# Forward-backward asymmetry

Forward-backward asymmetry $A_{\mathrm{FB}}$ is important observable in dilepton production **with a dual nature – electroweak and kinematical**:

$$A_{\mathrm{FB}} = \frac{\sigma^h_{\mathrm{F}} - \sigma^h_{\mathrm{B}}}{\sigma^h_{\mathrm{F}} + \sigma^h_{\mathrm{B}}}, \tag{14}$$

where according **J. Collins & D. Soper (1977)**:

- $\sigma^h_{\mathrm{F}}$ is “forward” cross section ($\cos\theta^* > 0$),
- $\sigma^h_{\mathrm{B}}$ is “backward” cross section ($\cos\theta^* < 0$).

In the Collins–Soper system $\cos\theta^*$ looks like:

$$\cos\theta^* = \mathrm{sgn}[x_2(t+u_1) - x_1(t_1+u)]\frac{tt_1 - uu_1}{M\sqrt{s(u+t_1)(u_1+t)}}.$$

# Forward, Backward (and Experimental) borders

For the case of nonradiative kinematics the $\cos\theta^*$ has especially simple view:

$$\cos\theta^* = \mathrm{sgn}[x_1 - x_2]\frac{u-t}{s} = \mathrm{sgn}\left[e^y - e^{-y}\right]\frac{(1+\mathcal{C})e^{-y} - (1-\mathcal{C})e^y}{(1+\mathcal{C})e^{-y} + (1-\mathcal{C})e^y}.$$

Solving $\cos\theta^* = 0$ we get **two conditions** for border dividing the regions of $\sigma_{\mathrm{F}}^h$ and $\sigma_{\mathrm{B}}^h$:

$$y = 0, \quad \mathcal{C} \equiv \cos\theta = \mathrm{th}\, y.$$

The CMS experimental condition $|\cos\theta| < \zeta^*$ is trivial but the second one $|\cos\alpha| < \zeta^*$ is rather sophisticated:

$$\cos\left(\arccos\frac{\cos\theta - \mathrm{th}\, y}{r} + \arcsin\frac{\sin\theta\,\mathrm{th}\, y}{r}\right) = \pm\xi^*,$$

where

$$r = \sqrt{1 - 2\cos\theta\,\mathrm{th}\, y + \mathrm{th}^2\, y}.$$

# Forward, Backward (and Experimental) regions

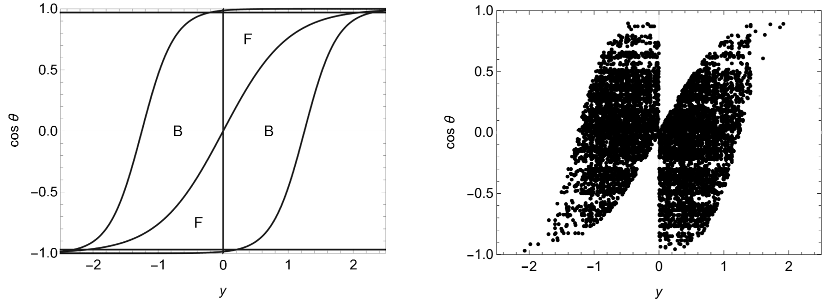


Figure 7: Left – Forward, Backward and CMS regions in $y$ and $\cos\theta$ variables (**borders are**: $y = 0$, $\cos\theta = \operatorname{th} y$, $\cos\theta = \pm\zeta^*$, and $\cos\alpha = \pm\zeta^*$, where $\zeta^* \approx 0.9866$),
right – the points sampled by Monte-Carlo generator of VEGAS **for Backward CMS region**.

# Additive relative corrections to $A_{\mathrm{FB}}$

Let 0 denotes the Born DY contribution, and for adiitional effect we use $c$:

$$c = \mathrm{NLO\ EW\ DY}, \mathrm{NLO\ QCD\ DY}, \mathrm{NLO}\ \gamma\gamma, \mathrm{IE}.$$

Corrected forward-backward asymmetry is defined as follows

$$\begin{aligned} A^c_{\mathrm{FB}} &= \frac{\sigma^0_{\mathrm{F}} + \sum_c \sigma^c_{\mathrm{F}} - \sigma^0_{\mathrm{B}} - \sum_c \sigma^c_{\mathrm{B}}}{\sigma^0_{\mathrm{F}} + \sum_c \sigma^c_{\mathrm{F}} + \sigma^0_{\mathrm{B}} + \sum_c \sigma^c_{\mathrm{B}}} = \\ &= \frac{\sigma^0_{\mathrm{F}} - \sigma^0_{\mathrm{B}}}{\sigma^0_{\mathrm{F}} + \sigma^0_{\mathrm{B}}} \times \frac{1 + \sum_c \delta^c_-}{1 + \sum_c \delta^c_+} = \\ &= A^0_{\mathrm{FB}} \times \frac{1 + \sum_c \delta^c_-}{1 + \sum_c \delta^c_+}, \end{aligned} \tag{15}$$

where

$$\delta^c_+ = \frac{\sigma^c_{\mathrm{F}} + \sigma^c_{\mathrm{B}}}{\sigma^0_{\mathrm{F}} + \sigma^0_{\mathrm{B}}}, \quad \delta^c_- = \frac{\sigma^c_{\mathrm{F}} - \sigma^c_{\mathrm{B}}}{\sigma^0_{\mathrm{F}} - \sigma^0_{\mathrm{B}}}.$$

# Dependance of $\delta^c_\pm$ on quark mass

| $n$ | $M_1$,TeV | $M_2$,TeV | $\delta^c_+$ | | | $\delta^c_-$ | | |
|---|---|---|---|---|---|---|---|---|
| | | | $\delta^{\rm ex}_+$ | $\delta^{\rm LL}_+$ | $\delta^{\rm gIE}_+$ | $\delta^{\rm ex}_-$ | $\delta^{\rm LL}_-$ | $\delta^{\rm gIE}_-$ |
| $-3$ | 0.106 | 0.12 | 8.139 | 8.070 | $-0.383$ | 5.257 | 5.128 | $-0.253$ |
| $-2$ | | | 6.771 | 6.694 | $-0.376$ | 4.375 | 4.199 | $-0.248$ |
| $-1$ | | | 5.393 | 5.322 | $-0.378$ | 3.479 | 3.302 | $-0.250$ |
| 0 | | | 4.019 | 3.951 | $-0.364$ | 2.590 | 2.426 | $-0.248$ |
| $-3$ | 0.51 | 0.60 | 4.185 | 4.101 | $-0.244$ | 3.710 | 3.632 | $-0.255$ |
| $-2$ | | | 3.544 | 3.458 | $-0.243$ | 3.130 | 3.057 | $-0.259$ |
| $-1$ | | | 2.902 | 2.816 | $-0.242$ | 2.560 | 2.483 | $-0.254$ |
| 0 | | | 2.259 | 2.173 | $-0.240$ | 1.984 | 1.908 | $-0.254$ |
| $-3$ | 1.0 | 1.2 | 2.812 | 2.757 | $-0.206$ | 2.829 | 2.791 | $-0.236$ |
| $-2$ | | | 2.392 | 2.337 | $-0.207$ | 2.399 | 2.364 | $-0.240$ |
| $-1$ | | | 1.972 | 1.918 | $-0.206$ | 1.969 | 1.936 | $-0.243$ |
| 0 | | | 1.553 | 1.498 | $-0.205$ | 1.545 | 1.509 | $-0.240$ |
| $-3$ | 3.0 | 6.5 | 1.240 | 1.219 | $-0.144$ | 1.505 | 1.499 | $-0.184$ |
| $-2$ | | | 1.059 | 1.039 | $-0.144$ | 1.284 | 1.280 | $-0.185$ |
| $-1$ | | | 0.880 | 0.859 | $-0.144$ | 1.064 | 1.060 | $-0.186$ |
| 0 | | | 0.699 | 0.679 | $-0.144$ | 0.843 | 0.840 | $-0.186$ |

$$m_q = 10^n m_u, \quad n = (-3, -2, -1, 0), \quad m_u = 0.06983 \text{ GeV}$$

# Relative corrections $\delta_+$ for Run3 of CMS LHC

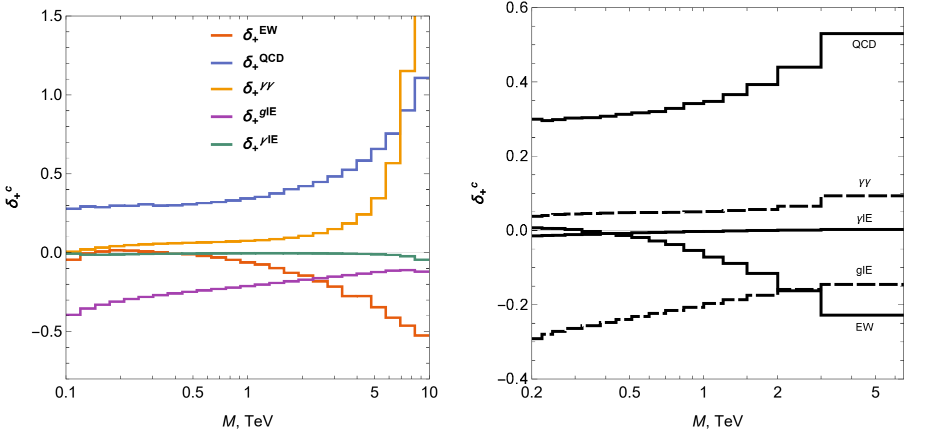


Figure 8: Additive relative corrections $\delta_+$ (left – MRST'04, right – NNPDF'24) for Run3 of CMS LHC ($\mu^+\mu^-$-production, $|y| < 2.5$).

# Relative corrections $\delta_-$ for Run3 of CMS LHC

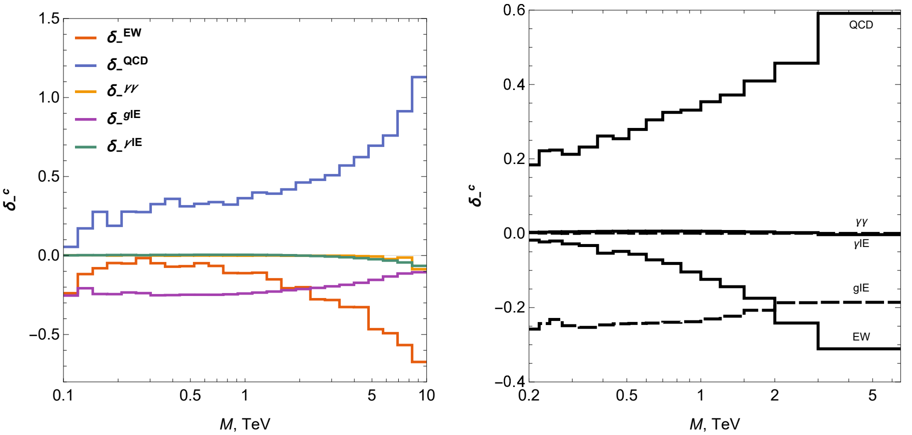


Figure 9: Additive relative corrections $\delta_+$ (left – MRST'04, right – NNPDF'24) for Run3 of CMS LHC ($\mu^+\mu^-$-production, $|y| < 2.5$).

# Net effect for relative corrections (Run3 of CMS LHC)

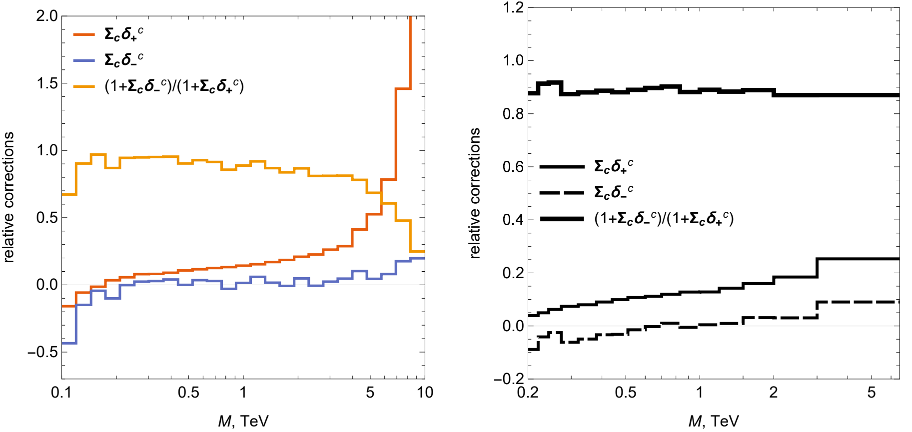


Figure 10: Total relative corrections (left – MRST'04, right – NNPDF'24) for Run3 of CMS LHC ($\mu^+\mu^-$-production, $|y| < 2.5$).

# Net effect for $A_{\mathrm{FB}}$ (Run3 of CMS LHC)

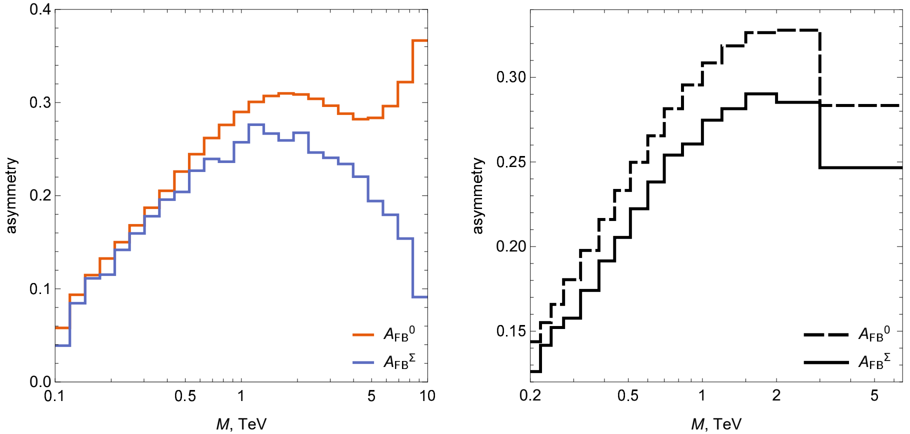


Figure 11: Forward-backward asymmetry $A_{\mathrm{FB}}$ (left – MRST'04, right – NNPDF'24) for Run3 of CMS LHC ($\mu^+\mu^-$-production, $|y| < 2.5$).

# Conclusions

- **The $g$ and $\gamma$ Inverse Emission** in dilepton production has been studied. It has been ascertained that the considered in Run 3 region IE effect changes the cross sections and $A_{\rm FB}$ **significantly**.
- **The net result** (NLO EW DY + NLO QCD DY + NLO $\gamma\gamma$-fusion + IE) to $A_{\rm FB}$ has been studied using **additive relative corrections technics**.
- The results are published in:
  - $g$ Inverse Emission – V. A. Zykunov, Phys. At. Nucl. **88**, 81 (2025),
  - $\gamma$ Inverse Emission – V. A. Zykunov, e-Print: 2506.03736 [hep-ph].

# Acknowledgement


- I am grateful to Organizers of this Seminar for happy possibility to take part.
- I would like to thank the **RDMS CMS group** members for the stimulating discussions and **CERN (CMS Group)** for warm hospitality during my visits.
- This work was supported by the **Convergence-2025** Research Program of Republic of Belarus (Microscopic World and Universe Subprogram).
- The numerical calcualtion was performed partically by **“HybriLIT”** of the Laboratory of Information Technologies of JINR.